

# Improved Platform Design for Organic Particle Detection using Buried Channel Waveguides

Thomas Wall

Department of Electrical and Computer Engineering  
Brigham Young University  
Provo, UT 84602  
thomas.wall@byu.edu

**Abstract**—This paper discusses the ARROW biosensor fabricated at Brigham Young University. The biosensor is integrated optofluidic device that is capable of individual organic particle detection. The biosensor was included in the Biological and Life Detection (BOLD) mission to Mars proposal for use in sensing any organic material left in the soil on Mars. The paper discusses the need for a high sensitivity for the biosensor and discusses on major design change that will improve the biosensor’s performance – changing the ridge waveguide used historically to a buried channel waveguide. The buried channel waveguide protects the waveguide from any detrimental water absorption within the waveguide and improves waveguide throughput over time.

## I. INTRODUCTION

Optofluidic devices are finding an increasing number of applications in today’s world. Many of the applications involve the sensing of organic particles present within a liquid solution. Many optofluidic devices are being engineered for this type of organic particle detection to be used in the medical field. They can sense a wide range of organics, from cancer cells, to viruses, to bacteria [1]. However, these devices can also find use outside of the medical field.

A major example of one such different use is the inclusion of an optofluidic biosensing device in a proposed life-searching mission to Mars, titled the Biological and Life Detection (BOLD) mission to Mars [2]. The optofluidic device included in the BOLD mission to Mars proposal is a biosensor that integrates two different types of optofluidic waveguides on a 1 cm x 1 cm silicon substrate, allowing for the optical probing of micro-volume liquid samples for any individual organic particles. The device proposed is suitable for the mission for several reasons. First, the device is very small and light weight. Any space travel is confined to very limited space and weight restrictions. The small size of the biosensor fits these limitations. Second, the

device is relatively low power. The power used to perform organic particle sensing is minimal and realistic for use on Mars. Third, the testing process is simple – mix soil samples into liquid solutions containing standard intercalating dyes and send the sample through the biosensor. The process can be automated and run without any human involvement.

This optofluidic biosensor is being developed at BYU by the Hawkins Biooptofluidics research group working in collaboration with the Schmidt group from UCSC. The biosensor makes use of a hollow anti-resonant reflecting optical waveguide (ARROW) in order to integrate guided light with fluidic samples and is termed by the group the ARROW biosensor [3-5]. This paper discusses this ARROW biosensor and how it works for biosensing, and then focuses on an important design change that increases the biosensor’s sensitivity and also improves its environmental stability. This change is the introduction of buried channel waveguides into the biosensor.

## II. THE ARROW BIOSENSOR

The ARROW biosensor is an optofluidic device capable of sensing individual organic particles [6]. Fig. 1a shows a cartoon schematic of the basic structure of the ARROW biosensor. The light blue channel in the schematic represents the hollow ARROW waveguide that is integrated on to the biosensor. This waveguide uses light interference effects in order to guide light through a low index, hollow channel [7].

The liquid sample to be tested must be mixed with a solution of intercalating dyes before it is introduced into the hollow channel via two reservoirs attached to the sensor. The intercalating dyes embed themselves into any DNA or RNA particles present in the liquid sample and once attached will fluoresce or emit light when excited by a certain wavelength of light. The ARROW

biosensor typically uses dyes that fluoresce at 488 nm or 635 nm.

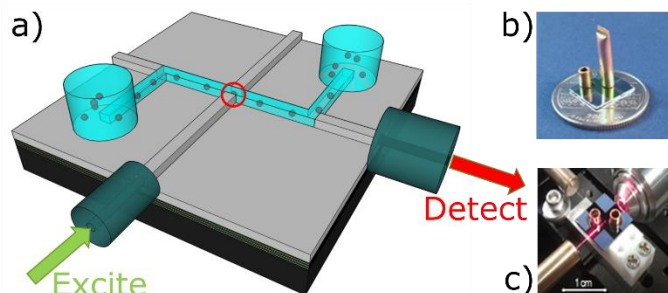


Figure 1: a) Schematic of the ARROW biosensor. The hollow core ARROW waveguide is shown in blue. The red circle indicates the excitation point where particles are excited optically. b) Finished ARROW biosensor resting on a quarter to indicate size. c) ARROW biosensor setup for a sensing experiment.

Once the liquid sample is ready and introduced into the reservoir, a pressure is applied to flow the sample through the hollow core ARROW waveguide. The hollow core waveguide is perpendicularly intersected by a standard solid core waveguide that has a constant intensity of laser light coupled into it from off chip. As particles flow through the hollow core waveguide and past the intersection point, the laser light excites any dyes embedded in DNA. These dyes give off a signal that is guided down the hollow core ARROW waveguide and off chip to be detected. Any dye molecules that have not attached to DNA will give off no signal. Using this method a liquid sample can be probed for the presence of any organic material within the sample.

It is important to note that the signal given off by each intercalating dye molecule attached to DNA is relatively small. A significant effort must be made in order to maintain a high enough signal after the light has been guided off chip. There are many loss factors that must be limited in order to allow for organic particle sensing using this platform. As always, the more improvements that can be made to the device, the better performance that can be expected. An important loss factor in the ARROW biosensor is the optical loss in the waveguides, specifically the solid core waveguides used in the device. The next section discusses the initial design for these solid core waveguides and a change that was made in order to improve performance.

### III. BURIED CHANNEL WAVEGUIDES

The solid core waveguides used in the ARROW biosensor were originally made using the ridge waveguide design, shown in Fig. 2a. However, a new

design, buried channel waveguides (BCWs), has been investigated due to a major problem inherent to the ridge waveguide design. A typical BCW design is shown in Fig. 2b. The difference in design is that the BCW design incorporates a thick top cladding layer over the guiding core of the waveguide [8, 9]. The ridge waveguide is designed to guide light within the ridge, which is completely exposed to its environment. The ridge waveguide design would work just fine if the waveguides environment did not affect the waveguide's performance; however, it is shown that water absorbed into the waveguide from its environment can greatly affect the waveguide's performance.

The solid core waveguides used in the ARROW biosensor are typically made using silicon dioxide ( $\text{SiO}_2$ ) deposited using a vapor phase deposition known as plasma enhanced chemical vapor deposition (PECVD). It is well known that  $\text{SiO}_2$  deposited via PECVD absorbs water from its atmosphere [10, 11]. It is also well known that as water absorbs in the  $\text{SiO}_2$  it will cause the refractive index of the  $\text{SiO}_2$  to increase. It has been shown that the index will increase as much as 1.8% its original value [12].

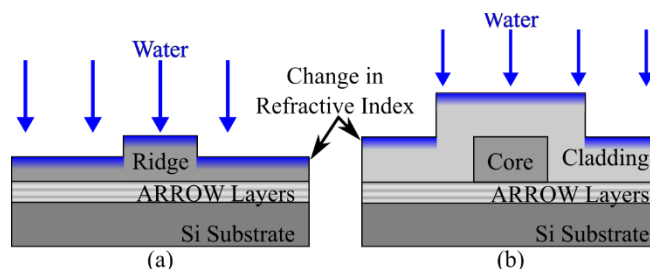


Figure 2: Schematic of a) a ridge waveguide and b) BCW waveguide. The figure shows where water will absorb into the waveguides with blue color. The refractive index will increase where water absorbs into the waveguide.

Fig. 2 illustrates a major problem with the ridge waveguide design. Water from the atmosphere will absorb directly into the guiding portion of the waveguide. Water absorption causes the refractive index to change in this sensitive area and the waveguide begins to perform different than expected. In contrast, the BCW design buries the light guiding core of the waveguide deep under a protective cladding layer. While the cladding is made of the  $\text{SiO}_2$ , as well, and also absorbs water, the layer helps to keep any water absorption far away from the critical guiding area of the waveguide.

### IV. EXPERIMENT

Several ridge waveguide and BCW waveguide samples were fabricated in order to test their resilience when exposed to high water environments. The waveguides were all made using standard

microfabrication processes in the BYU cleanroom. The ridges were designed to be  $3\ \mu\text{m}$  tall and  $12\ \mu\text{m}$  wide. The BCWs were designed to have a core height of  $6\ \mu\text{m}$  and a width of  $12\ \mu\text{m}$ . These dimension were used because they represent the actual waveguide dimensions that would be used on the ARROW biosensor. Fig. 3 shows scanning electron micrographs of a ridge waveguide and a BCW waveguide.

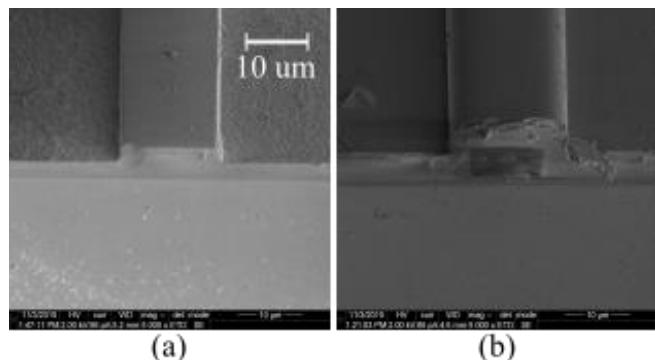


Figure 3: SEMs of a) ridge waveguide and b) BCW waveguide.

An optical table setup was built at BYU and used to test and characterize the waveguides. The optical setup was capable of characterizing the waveguides in three different ways. First, the waveguides' total optical throughput was measured by collecting light from the waveguide in a photodiode. Second, top view images of the waveguides were taken while laser light was being couple into them. This top view image was very useful for understanding much of the waveguides' behavior throughout the experiment. Third, a side view image of the waveguide allowed for imaging of the waveguides' modal behavior.

Upon completion of fabrication, the waveguides were removed from the BYU cleanroom and immediately characterized on this optical setup. The waveguides were then immersed in an  $85^\circ\text{C}$  water soak. The water soak helped to accelerate any effects that would occur in the waveguides due to water absorption. The temperature of  $85^\circ\text{C}$  was chosen because it was convenient to keep the water well below  $100^\circ\text{C}$  to avoid all of the water evaporating away.

## V. RESULTS

This section reports on the results of the experiment described above. Fig. 4c is a graph of the optical throughput of the waveguides throughout the course of the experiment. Day 0 represents the throughput of the waveguide before they were immersed in an  $85^\circ\text{C}$  water soak. The data presented is an average of 3 BCW

waveguides and 5 ridge waveguides. The error bars indicate a 12% error and are based on the ability of the setup to measure the throughput of the same device several times. The BCW data is represented with a solid line and the ridge waveguide data is depicted using a dashed line.

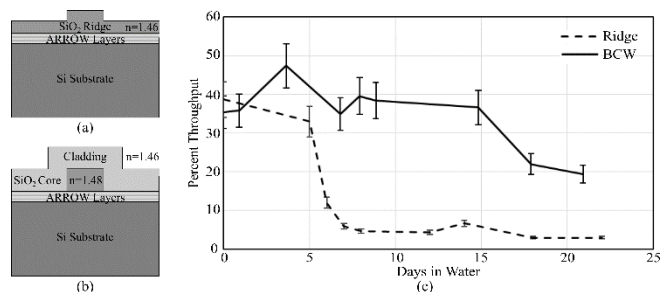


Figure 4: (a) Ridge waveguide design profile. (b) Buried channel waveguide (BCW) design profile. (c) Plot of the average percent optical throughput vs. days soaking in  $85^\circ\text{C}$  water for both the BCWs (solid line) and ridge waveguides (dashed line).

Fig. 4 shows that the percent optical throughput of the ridge waveguides decreased drastically throughout the experiment. By day 7 the optical throughput had dropped below 5%, representing a drop of almost 90% in signal from its original value. The BCW waveguide samples fared somewhat better than the ridge samples. The BCWs remained above 20% throughput even after 20 full days of soaking in the  $85^\circ\text{C}$  water. This is a drop of only  $\sim 30\%$  from their original value before being exposed to water.

Top view images were also taken of the waveguides every time the optical throughput was measured. The top view images help explain the large decrease in throughput for the ridge waveguides. Fig. 5a shows a ridge waveguide before being exposed to water (top) and the same ridge waveguide after 20 days in the  $85^\circ\text{C}$  water soak (bottom). The bottom image shows that the light is no longer being well confined to the core or ridge of the ridge waveguide. After spending time in water, much of the light in the ridge waveguide escapes the core and scatters out to the side. Fig. 5b integrates the light in these images and shows in dark red where the core of the waveguide actually resides.

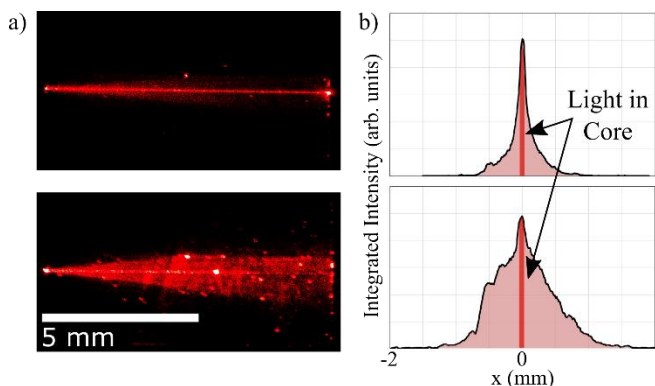


Figure 5: a) Top view images of the same ridge waveguide while being excited by 635 nm light on (top) day 0 and on (bottom) day 22. b) Integrated profile of the images to the left. The darker red section represents the width of the core and where the light should be guiding.

This same effect was not seen in the BCW waveguide samples. After 22 days soaking in 85°C water, the BCW waveguides still had a large percentage of light guiding within the core and not scattering out the side. In Fig. 6 the y-axis is the percent light that is guiding within the core of the waveguide. The value graphed is the last value tested, around day 22. The graph shows that on that day there was still around 95% of the light guiding in the core of the BCWs while there was less than 50% in the cores of the ridge waveguides.

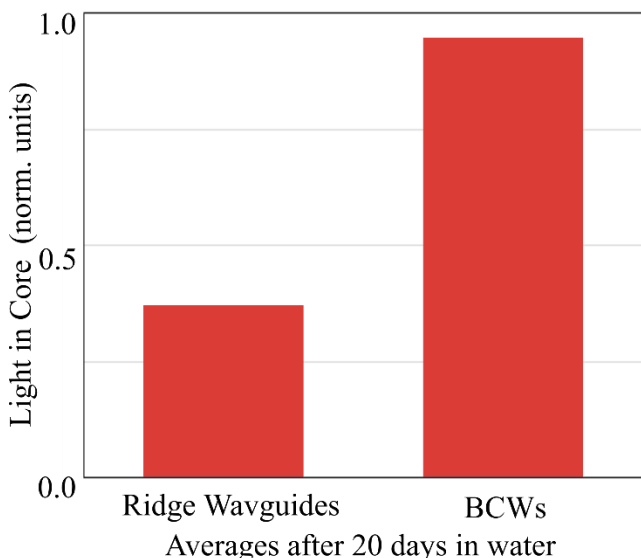


Figure 6: Amount of light guiding within the core after 20 days normalized to values from day 0.

Side view images were also taken of the waveguides in order to study their modal behavior. It was found that the mode of the ridge waveguide completely changed over the course of the experiment. Before exposure to water the mode of the ridge waveguide resided right in

the center of the ridge; however, after being exposed to water the mode began to move up, towards the surface of the waveguide. The mode of the BCW waveguide samples did not change throughout the experiment. It guided in the core on day 0 and on day 22 was still guiding in the core.

## VI. DISCUSSION

As shown above the ridge waveguide samples tested in this experiment began to perform poorly as waveguides after being exposed to an aqueous environment while the BCW waveguide samples were able to remain much more stable. This section discusses why the ridge waveguides were more susceptible to detrimental effects from water absorption. This section also discusses the possible improvement in biosensing by incorporating BCW waveguides into actual ARROW biosensors.

It is mentioned above that water absorbing into SiO<sub>2</sub> causes the refractive index of the SiO<sub>2</sub> to increase. The increase is not extreme, only around 1.8% after complete saturation. However, in optical waveguides, any change in refractive index can cause the waveguides to function completely different than before. In order to better understand the behavior portrayed by these ridge waveguide, we used software in order to simulate what might happen to the waveguide upon water absorption in the top of the waveguide (FIMMWAVE). Figure 7 shows some images from that simulation.

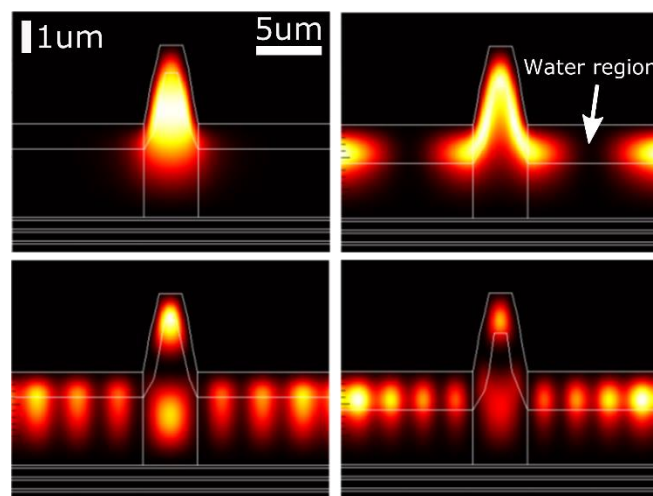


Figure 7: FIMMWAVE simulation of ridge waveguide with a 2 μm deep top water layer. Each image represents a possible guiding mode for the waveguide.

The ridge was simulated with a 2 μm water saturated layer. This layer was given a refractive index 1.8%

higher than the rest of the waveguide. Fig. 7 shows several of the possible modes that can guide in that ridge waveguide. It shows that the high index layer raises the mode of the waveguide up towards the surface. Also, the waveguide begins to have modes that fan out to the left and right of the ridge. In essence, the simulations match what was seen in the experiment. A high index top layer in the ridge waveguide causes the ridge waveguide to behave non-ideally. The waveguide begins to let light scatter out of the sides and causes the percent optical throughput of the waveguide to decrease dramatically.

The BCW maintains its throughput because the water does not penetrate deep enough into the protective cladding layer of the waveguide to greatly affect the waveguiding properties of the waveguide. It must be noted however, that the throughput of the BCW waveguide samples did drop, as well, just not nearly as much. The reason for this is that the water penetrated deep enough into the top cladding layer to cause some of the light power to escape out of the waveguide. This problem can be fixed by simply increasing the thickness of the protective top cladding layer.

This experiment was run with individual waveguides that were not integrated into a biosensor. The results clearly show that the BCW waveguides would far outperform the ridge waveguides if they were integrated into the ARROW biosensor platform. This can be done quite easily and is future work that should be done in

order to show how an introduction of BCW waveguides into the ARROW biosensor improves the sensitivity of the biosensor. It has been found with the ARROW biosensors made using ridge waveguides can perform poorly over time. The BCW waveguides will make the ARROW biosensors last much longer.

## VII. CONCLUSION

The ARROW biosensor is an optofluidic device that is fabricated and researched by the Biooptofluidics group under Dr. Hawkins at Brigham Young University in collaboration with Dr. Holger Schmidt's group at the University of California, Santa Clara. The biosensor was included in the BOLD mission to Mars proposal due to its small size, low power, and individual organic particle sensing capability. In order for the ARROW biosensor to have its highest possible sensitivity and worth for such an application all optical losses in the device must be minimized. One important improvement in the ARROW biosensor is replacing the ridge waveguides used historically in the biosensor with BCW waveguides. The BCW design helps protect the waveguides from their environment. They especially help prevent detrimental water absorption in the waveguide. Water absorption causing problems in the ARROW biosensor has been a major problem for the biosensors in the past and the introduction of BCWs will mitigate that problem.

- [1] H. Schmidt and A. R. Hawkins, "The photonic integration of non-solid media using optofluidics," *Nature Photonics*, vol. 5, pp. 598-604, Oct 2011.
- [2] D. Schulze-Makuch, J. N. Head, J. M. Houtkooper, M. Knoblauch, R. Furfaro, W. Fink, *et al.*, "The Biological Oxidant and Life Detection (BOLD) mission: A proposal for a mission to Mars," *Planetary and Space Science*, vol. 67, pp. 57-69, 7// 2012.
- [3] D. L. Yin, D. W. Deamer, H. Schmidt, J. P. Barber, and A. R. Hawkins, "Single-molecule detection sensitivity using planar integrated optics on a chip," *Optics Letters*, vol. 31, pp. 2136-2138, Jul 15 2006.
- [4] D. Ozelik, J. W. Parks, T. A. Wall, M. A. Stott, H. Cai, J. W. Parks, *et al.*, "Optofluidic wavelength division multiplexing for single-virus detection," *Proceedings of the National Academy of Sciences*, vol. 112, pp. 12933-12937, 2015.
- [5] H. Cai, J. Parks, T. Wall, M. Stott, A. Stambaugh, K. Alfson, *et al.*, "Optofluidic analysis system for amplification-free, direct detection of Ebola infection," *Scientific reports*, vol. 5, 2015.
- [6] D. L. Yin, E. J. Lunt, M. I. Rudenko, D. W. Deamer, A. R. Hawkins, and H. Schmidt, "Planar optofluidic chip for single particle detection, manipulation, and analysis," *Lab on a Chip*, vol. 7, pp. 1171-1175, 2007.
- [7] M. A. Duguay, Y. Kokubun, T. L. Koch, and L. Pfeiffer, "Antiresonant Reflecting Optical Wave-Guides in SiO<sub>2</sub>-Si Multilayer Structures," *Applied Physics Letters*, vol. 49, pp. 13-15, Jul 7 1986.
- [8] G. Grand, J. P. Jadot, H. Denis, S. Valette, A. Fournier, and A. M. Grouillet, "Low-Loss Pecvd Silica Channel Wave-Guides for Optical Communications," *Electronics Letters*, vol. 26, pp. 2135-2137, Dec 6 1990.
- [9] G. Grand, J. P. Jadot, H. Denis, S. Valette, A. Fournier, and A. M. Grouillet. (1990, Low-loss PECVD silica channel waveguides for optical communications. *Electronics Letters* 26(25), 2135-2137. Available: [http://digital-library.theiet.org/content/journals/10.1049/el\\_19901375](http://digital-library.theiet.org/content/journals/10.1049/el_19901375)

- [10] S. Wendt, M. Frerichs, T. Wei, M. S. Chen, V. Kempter, and D. W. Goodman, "The interaction of water with silica thin films grown on Mo(112)," *Surface Science*, vol. 565, pp. 107-120, Sep 10 2004.
- [11] A. Brunet-Bruneau, S. Fisson, G. Vuye, and J. Rivory, "Change of TO and LO mode frequency of evaporated SiO<sub>2</sub> films during aging in air," *Journal of Applied Physics*, vol. 87, pp. 7303-7309, May 15 2000.
- [12] M. Stott, T. Wall, D. Ozcelik, J. Parks, G. G. Meena, E. Hamilton, *et al.*, "Silicate Spin-on-Glass as an Overcoat Layer for SiO<sub>2</sub> Ridge Waveguides," in *CLEO: 2015*, San Jose, California, 2015, p. JTh2A.29.